Microstructural Path Analysis of Martensite Dimensions in FeNiC and FeC Alloys

José Roberto Costa Guimarães[a]*, Paulo Rangel Rios[a]

[a]*Escola de Engenharia Industrial Metalúrgica de Volta Redonda, Universidade Federal Fluminense - UFF, Av. dos Trabalhadores, 420, CEP 27255-125, Volta Redonda, RJ, Brasil*

The properties of steels that undergo martensite transformation after or during processing depend on characteristics and arrangement of martensite units within the microstructure. In this work, the global microstructure descriptors of martensite transformation are related to the individual dimensions of the martensite units, the "intrinsic dimensions", – radius, thickness and aspect ratio – compensated for interactions among those units. In other words, the dimensions a martensite unit would have if it grew without impingement. This is accomplished by means of the microstructural path method. The methodology was applied to experimental data of martensite transformation in FeNiC and FeC alloys. The analysis of martensite dimensions permitted observing that the microstructural path of martensite includes a thermally activated step. We conclude that this thermally activated step does not mean that martensite itself has thermally activated growth step but that arrest of the martensite thickening process, owing to dislocation interaction with the interface motion may be thermally activated.

Keywords: *martensitic phase transformation, microstructure, analytical methods*

1. Introduction

The microstructure of martensite is of fundamental and practical interest because many steels of industrial importance derive their engineering properties from martensite transformation during or after processing. Historically, the martensite transformation in steels has been deemed time-independent ("athermal"). The transformation proceeds upon cooling by successive nucleation events assisted by autocatalysis[1,2] that influences the intra-grain transformation, i. e. "fill-in", as well as promotes inter-grain transformation, i. e. "spread"[1,2]. The propagation of martensite comprising nucleation and growth is nucleation controlled. The growth is usually very fast. Growth stops when the unit reaches a certain size delimited by impingement and/or by the austenite plasticity[3,4]. Coarsening is not observed. Martensite is a displacive transformation so that the product-units cannot cross high-angle boundaries, thus they remain confined to the grains where they propagate. Nonetheless, the midribs of two impinging units may cross if the stress field on impingement suffices to induce nucleation of the same martensite variant across the impinged unit as observed by Okamoto and co-workers[5] in a Fe- 31wt%Ni-0.28wt%C alloy.

The elastic strain energy of a martensite unit, proportional to its aspect ratio, has major influence on the microstructure development. This energy is very high, and relaxation occurs by plastic deformation within the martensite, the invariant-shear, in the surrounding austenite as well as by the transformation of self-accommodating groups of martensite-units[6]. As consequence of the latter, the aspect ratio of the units observed in a microstructure tends to be coarser than expected from propagation intrinsic mechanisms.

These intrinsic aspects of martensite growth have been considered from different points of view[7-15]. However, the linkage to a formal description of the progress of martensite transformation as a function of the leading variable still deserves effort, minding the microstructural complexity of martensite, an example of which is shown in Figure 1.

Likewise other phase transformations, the progress of the martensite is generally expressed by the volume fraction transformed as a function of a variable related to the progress or advancement of the transformation, such as, temperature, strain or time. Nonetheless, that is not always sufficient for process-design, or for delving mechanisms, or for advanced-materials development. A better approach was proposed by DeHoff[16]. DeHoff introduced the concept of microstructural path to characterize the sequence of states that a system goes through during a phase transformation. His idea was subsequently developed into a fully-fledged analytical methodology, the microstructural path method, MPM, by Vandermeer and co-workers[17]. The microstructural path method has been employed in recrystallization as well as in diffusional transformation studies. The microstructural path function for recrystallization is represented by $\Psi(S_V, S_V) = K_\Psi$ where V_V is the volume fraction of the product phase, S_V is the area per unit volume of product-matrix interfaces, and K_Ψ is a parameter linked to the mechanism of the transformation. A similar approach was used by the present authors to analyze the autocatalytic "spread" of martensite from a few initially transformed grains to their untransformed neighbors[18,19]. In the present work, we move another step to apply the microstructural path method to consider intrinsic aspects of the martensite transformation.

*e-mail: prrios@id.uff.br

2. Formal Description of Martensite Microstructural Path

The microstructural path method may be expressed in real or in "extended space". The latter is a concept due to (JMAK) Johnson-Mehl, Avrami and Kolmogorov[20-22] to analyze classical nucleation and growth of shape-preserved transformations that are randomly-nucleated. In the present work, we apply the "extended space" concept to characterize the martensite transformation in the absence of interaction with other units to relax the shape strain. Recently, the JMAK type problem has received rigorous mathematical treatment falling within the class of the so-called "birth-and-growth" processes[23,24]. Recently, Rios & Villa[23] revisited and generalized the early JMAK theory. Rios and Villa showed that Poisson point processes and Boolean models are the essential mathematical ingredients underlying modern treatment of JMAK process. Nonetheless, in what follows, even though we bear in mind Rios and Villa results, we continue to adopt the classical terminology of the Metallurgy and Materials Science field.

The martensite product-units exhibit well defined morphologies and crystallographic habit, so that shape is preserved. The initial martensite nucleation is promoted by defects ("embryos") pre-existent in the austenite, and proceeds autocatalytically. That is, the first unit to propagate yields a local transformation-burst that *fills-in* that austenite grain. The impingement of a unit on a grain boundary is capable of *spreading* the transformation into next grain and so forth. Such *spread-event* results in a cluster of partially transformed grains. Since those pre-existent embryos are scarce and randomly distributed throughout the austenite grains[25], randomness also underlies the clusters resultant from the initial propagations at temperature, T. The crystallographic-variants of the martensite units observed in a grain are delimited by variant-selection to accommodate transformation strains[6]. Nevertheless, since neighbor grains have different orientations, aligned martensite microstructures are hardly observed in real space so that it is admissible that the randomness of those embryos that initiate different spread-events also underlies the martensite units therein - see
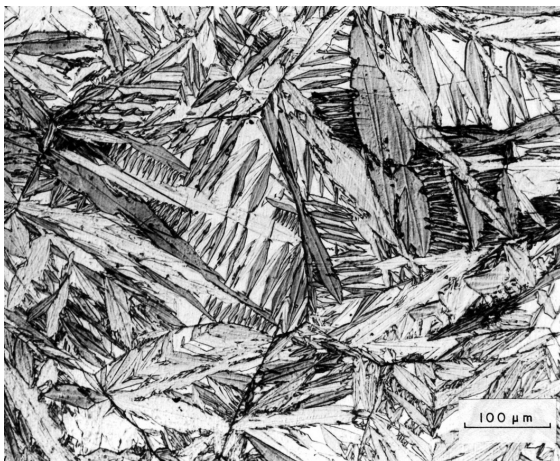

Figure 1. Microstructure of martensite transformation in Fe-31wt%Ni-0.02wt%C transformed by cooling into liquid nitrogen. Micrograph obtained by J. R. C. Guimarães.

Figure 1. Therefore, although the martensitic transformation might not entirely fulfill the JMAK assumptions[20-22], their equations will be used here as reasonable approximations. See Nok Chiu et al.[24] for a more in depth mathematical discussion of usage of Boolean models in practical situations. Admittedly, the results therefrom derived here will need a careful evaluation.

Henceforth, consider the microstructure of a material containing N_V disc-shaped martensite units per unit volume comprising the volume fraction transformed, V_V, and the volume density of martensite-austenite interfaces, S_V. These two descriptors are readily obtainable by point and lineal counting on the actual microstructure. The subscript "i" is used to mark descriptors of the dimensions of a martensite unit in extended space that can be called "intrinsic dimensions". Proceeding, the extended volume fraction transformed, V_{VE}, as a function of the N_V units is

$$V_{VE} = v_i N_V \tag{1}$$

where v_i is the intrinsic volume of a martensite unit. For disc-shaped martensite,

$$v_i = \alpha_i \frac{\pi}{4} d_i^3 \tag{2}$$

where d_i and α_i are, respectively, the intrinsic diameter and the aspect ratio of a martensite unit formed at temperature T. Substituting Equation 2 into Equation 1, using JMAK's equation $V_V = 1 - \exp(-V_{VE})$, and rearranging terms

$$\alpha_i = \frac{4}{\pi} \frac{\ln(1-V_V)^{-1}}{d_i^3 N_V} \tag{3}$$

Since $t_i = d_i \cdot \alpha_i$,

$$t_i = \frac{4}{\pi} \frac{\ln(1-V_V)^{-1}}{d_i^2 \cdot N_V} \tag{4}$$

Recalling that $S_V = S_{VE}(1-V_V)$ where $S_{VE} = 2\pi r_i^2 N_V$, one obtains

$$\alpha_i = t_i/2r_i = \sqrt{2\pi N_V/S_V^3}(1-V_V)^{3/2}\ln(1-V_V)^{-1} \tag{5}$$

$$t_i = 2(1-V_V)\ln(1-V_V)^{-1}/S_V \tag{6}$$

and

$$d_i = \sqrt{2S_V/\pi N_V(1-V_V)} \tag{7}$$

Similarly to the microstructural path analysis conducted during recrystalization and/or diffusional phase transformations, the intrinsic dimensions correspond to the dimensions of a unit or of a single transformed region in the absence of impingement. In other words, the intrinsic dimensions represent how a martensite unit would develop in the absence of other units, that is, interacting only with its surrounding austenite.

Note that Equations 5 to 7 express different aspects of the microstructural path. Equations 5 and 7 contain the three descriptors: V_V, S_V, N_V, that characterize the "state of the system" made of austenite and martensite units, whereas Equation 6 on V_V and S_V is a "partial" path function pertaining to the thickening of the martensite units that follows the propagation of the unit's midrib.

3. Materials and Data

The data used here were scanned from the graphs in the referenced papers and digitized with a freeware software. These data were consolidated by reiteration and by averaging out small variations. Whereas the original data sources do not report error bars, experience with quantitative stereological techniques used in those works suggests that ±10% relative error is not an unreasonable estimate of errors associated with such measurements. Our reference material is a Fe-31wt%Ni-0.02wt%C[26-28] alloy. The Fe-1.86wt%C[29] alloy was also included in this analysis. The information provided by this alloy on high carbon martensite might be particularly useful because the high resistance to crashes exhibited by the modern low-alloy multiphase TRIP-aided steels is provided by the martensite transformation in the high-carbon retained austenite present in these materials[30]. Both the Fe-Ni-C and the Fe-C alloys transform at sub-zero temperatures, which allowed up-quenching for quantitative optical microscopy evaluation at room temperature. Standard methods were employed to determine S_V and V_V. The Fullman's[31] methodology was used to calculate N_V from planar sections. Fullman derived his equations for slender disks, this morphology was also the starting point of the derivations carried out above. In this way the derived equations are compatible with data obtained by Fullman's methodology. Further details about the experiments are available in the referenced works. Here the expressions "austenite grain intercept" or simply "grain intercept" are used to denote "mean intercept length of austenite grains".

Table 1 depicts data obtained from the Fe-Ni-C alloy with austenite grain intercept $d_\gamma = 0.142$ mm, transformed by quenching to different temperatures[26-28]. The data typical of the high-carbon Fe alloy with grain intercept $d_\gamma = 0.110$ mm also resulted from cooling. Table 2 depicts data published

in[29] along with the values of $S_V = 2V_V / \bar{t}$ calculated here by substituting $\bar{t} \cong \bar{r} \cdot \langle t/r \rangle$ assuming the mean aspect ratio of the martensite units $\langle t/r \rangle$ to be independent of the unit size. Data in Table 3 pertain to the initial transformation-burst typical of the Fe-31wt%Ni-0.02wt%C alloy with different grain-sizes ($d_\gamma = 0.027:0.142$ mm) cooled to the burst temperature, M_B, which coincided with the martensite start temperature. The temperature M_B of these materials exhibited small variation, so that we shall associate the variations of the microstructure descriptors to the different austenite grain-sizes. Tables 1-3 also depict values of the intrinsic parameters, indicated by the subscript "i", calculated by Equations 3-5 that were derived supposing martensite units shaped like thin discs.

4. Results

Inspection of data depicted in Tabels 1, 2 and 3 reveals that the intrinsic dimensions of the martensite formed in absence of mutual interactions conforms to the displacive aspect of martensite. The values r_i are larger than the actual mean plate radius, $\bar{r}$, yet shorter than $d_\gamma/2$. On the other hand, t_i is less than the actual mean thickness of the martensite units, $\bar{t}$, reflecting the absence of mutual accommodation of the shape-strains. The smaller values of α_i typical of the Fe-1.86wt%C compared with those of the Fe-31wt%Ni-0.02wt%C are consistent with the slender morphology of the high-C martensite. In addition, one acknowledges qualitative compatibility between the temperature variation of the intrinsic aspect ratio of the FeNiC martensite depicted in Tables 1-3 with the data reported in[32,33]– see Figure 2. The steeper temperature-variation of α_i in comparison with the mean semi-thickness to radius $\langle c/r \rangle$ ratio of the martensite units reported in Datta-Raghavan[32] and Visvesvaran[33] is due to the difference in the experimental methodology. In Datta-Raghavan[32] and Visvesvaran[33] the authors obtained the variation of $\langle c/r \rangle$ by using alloys with

Table 1. Fe-31wt%Ni-0.02wt%C alloy - Experimental and calculated microstructure descriptors for an austenite grain size equal to 0.142 mm[26-28].

Temperature, K	N_V, mm⁻³	V_V	S_V, mm⁻³	$\bar{t}$, mm	t_i, mm	$\bar{r}$ mm	r_i, mm	α_i
220 (M_S)	2725	0.23	30.54	0.015	0.013	0.034	0.048	0.133
213	11429	0.39	65.81	0.012	0.009	0.026	0.039	0.115
203	17416	0.54	77.51	0.014	0.009	0.022	0.039	0.115
188	29543	0.69	100.54	0.014	0.007	0.020	0.042	0.083
171	66046	0.75	172.67	0.009	0.004	0.021	0.041	0.049

Table 2. Fe-1.86wt%C - Experimental and calculated microstructure descriptors for an austenite grain size equal to 0.110 mm[29].

Temperature, K	N_V, mm⁻³	V_V	S_V, mm⁻³	$\bar{t}$, mm	t_i, mm	$\bar{r}$ mm	r_i, mm	α_i
220 (M_S)	15000	0.12	97.1	0.003	0.0024	0.023	0.0343	0.035
213	69000	0.27	320.3	0.002	0.0014	0.016	0.0318	0.022
203	214000	0.36	597	0.001	0.0010	0.011	0.0264	0.019
188	509000	0.51	919	0.001	0.0008	0.010	0.0241	0.017

Table 3. Fe-31wt%Ni-0.02wt%C ally - initial bursts – Experimental[26-28] and calculated microstructure descriptors with Equations 3-5.

$d\gamma$, mm	M_S, K	N_V, mm⁻³	V_V	S_V, mm⁻³	$\bar{t}$, mm	t_i, mm	$\bar{r}$ mm	d_i, mm	α_i
0.027	213	13910	0.035	18.5	0.005	0.004	0.0125	0.030	0.133
0.049	220	12500	0.05	40.3	0.002	0.002	0.014	0.046	0.043
0.064	222	10800	0.18	47.8	0.007	0.007	0.025	0.058	0.121
0.142	220	2725	0.23	30.5	0.015	0.013	0.034	0.096	0.135

different chemistries that transform at different temperatures, and also by mechanical stimulating their transformation above the natural M_S [32,33]. Whereas, in the present work JMAK's extended-space concept[20-22] was used to estimate the intrinsic dimensions of the martensite units formed in bulk polycrystalline-specimens of the reference-alloys cooled to temperatures below the martensite-start. The actual microstructure parameters, earlier obtained by standard quantitative optical microscopy, were compiled from the referenced works.

To proceed, mind that the substructure of lenticular-martensite observed in high-Ni FeNiC alloys comprises three regions: the midrib, the twinned region and the untwinned region near the martensite-austenite interface[8,14]. The midrib of the FeNiC lenticular-martensite is analogous to the fully twinned thin-plate martensite that forms at lower temperatures. The formation of this midrib precedes the development of the untwinned zone, which develops with the change in the the invariant shear from twinning to slip, attributed to local temperature raise[8]. It is worthy of note that the twinning-slip transition has also been observed in high carbon martensite[34].

It is worthy examining the temperature variation of the intrinsic ratio and of the intrinsic thickness of the martensite transformed in the two alloys. Decreasing the temperature (*T*) causes r_i and t_i to decrease – see Figure 3. Note that the r_i (square-markings) changes much less than t_i (circle-markings). This observation supports the view that the martensite propagation is not single-step. The midrib of lenticular-martensite is similar to thin-plate martensite that tends to grow with minimum disturbance within the surrounding austenite[15]. Moreover, sometimes a midrib is seen to penetrate an impinged unit until the boundary of the twinned zone. Readily noticed in the Fe-31wt%Ni-0.02wt%C[35], this fact supports the assertive that the development of the untwinned zone is considerably slower than that of a midrib[8]. Regarding the thickening of lenticular-martensite, it is pertinent recalling that although the austenite-martensite interface in lenticular-martensite cannot move conservatively[36], the high driving force attending the transformation should permit the interface to move fast "by forming point defects at sessile jogs or leaving dislocations inside the martensite plate"[37]. It is worthy of note that the approach used here does not allow direct inferences regarding the changes in the martensite substructure and its growth-mechanism. Nonetheless, it should be apparent that the dimensions of the martensite units reflect the growth-arrest that relates to plastic deformation in the surrounding austenite[38]. Thence, it is feasible that thermal processes may be involved in the formation and/or in the interaction of that plastic zone with the martensite-austenite interface. Bearing that in mind, the temperature variation of t_i may be analyzed with the help of Arrhenius plots. For this analysis, the temperature of the specimens is considered to be equal to that of the quenching medium. This is reasonable because the experimental conditions were such that[26-28] the volume of specimen was roughly 1/1000 of the volume of the quenching medium. The results of this analysis are seen in Figure 4. The linear regressions with high coefficients of determination, R^2=0.91-0.94, permitted to calculate apparent-energies values, which are compatible with deformation by dislocation motion. One

obtains similar activation energies: 1.1 10^{-20} J/event and 1.27 10^{-20} J/event, respectively from the FeNiC and from the FeC data. These small energy values are compatible with dislocation-processes, thus supporting the view that the
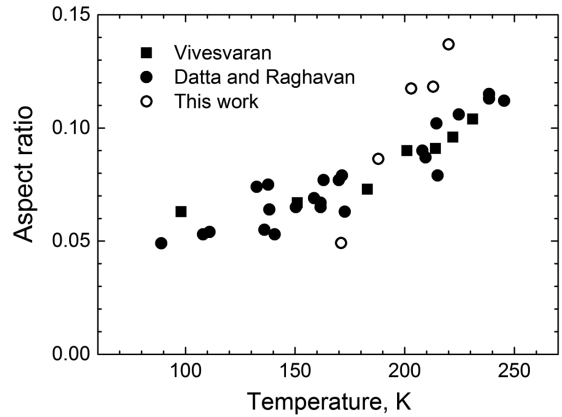

Figure 2. Comparison of the values of the martensite aspect ratio, mean half-thickness to radius of martensite units, in different alloys obtained from Datta & Raghavan[32] and Visvesvaran[33].
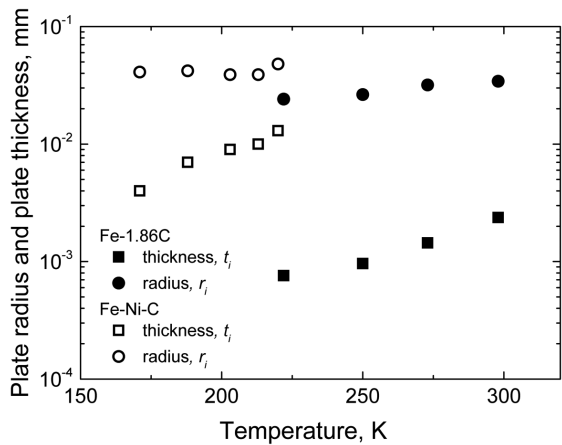

Figure 3. Intrinsic dimensions of martensite units in Fe-31wt%Ni-0.02wt%C[26-28] and Fe-1.86wt%C[29] quenched to different temperatures.
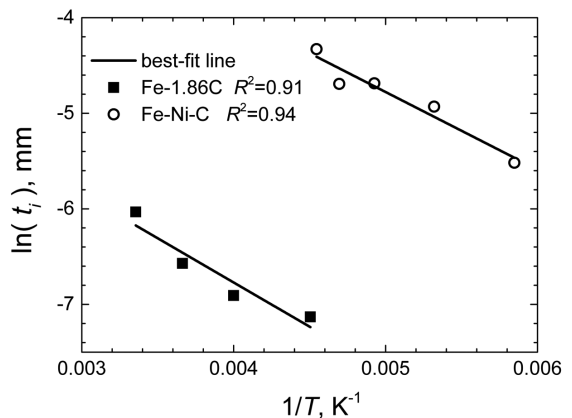

Figure 4. Arrhenius plot of intrinsic thickness of martensite as a function of the quenching temperature for data from Fe-31wt%Ni-0.02wt%C[26-28] and Fe-1.86wt%C[29] alloys.

intrinsic aspect-ratio of martensite carries the temperature dependence of the interaction of that plastic zone with the martensite-austenite interface. At present, it is accepted that dislocations from the plastic zone can be inherited and/or may be swept by the interface. Furthermore, as already mentioned above, the change in the invariant-shear typical of lenticular martensite has been attributed to local temperature raise[8].

The influence of the austenite grain size, d_γ, on the size of the transformed martensite relates to the displacive aspect of the transformation. This effect has been assessed with the data typical of the initial transformation-burst in the Fe-31wt%Ni-0.02wt%C shown in Table 3. These values of intrinsic diameter, $d_i = 2r_i$, and of the intrinsic-thickness, t_i, are graphed against d_γ in Figure 5. Larger units are formed in the coarser grained materials, as expected. Notable, t_i and d_i increase with increasing d_γ. In Figure 5 the line with slope 1 represents the situations in which $d_i = d_\gamma$. For $0.026 \leq d_\gamma \leq 0.064$ mm one has $d_i \approx d_\gamma$. This is consistent with the experimental fact that in our reference FeNiC alloy, the martensite units partition the austenite grains. In contrast, for $d_\gamma = 0.142$mm the value of $d_\gamma > d_i$ suggests a dragging effect of the austenite plasticity on the radial-growth of martensite[38]. The linear dependence of both r_i and t_i on d_γ highlighted in Figure 5 is consistent with the lack of a clear dependence of $\alpha_i = t_i/d_i$ on the austenite grain size, Table 3. Thence, in our reference material, the influence of temperature on α_i is overwhelming mainly through its influence on t_i, Figure 3.

5. Discussion

In the foregoing, the microstructure path descriptors V_i, S_V and N_V were used to analyze the temperature dependence of the dimensions of martensite in absence of self-accommodation. The decrease of the intrinsic aspect-ratio of martensite with the transformation temperature is in qualitative agreement with the data described in[32,33,39]. In the present work, the influence of thermal energy on the aspect ratio of martensite could be brought forth by analyzing martensite's microstructural path in extended space as a mean to compensate the observed unit-size for self-accommodation. The intrinsic thickness of martensite units typical of Fe-31wt%Ni-0.02wt%C and of Fe-1.86wt%C thus obtained could be empirically represented with high coefficients of determination in Arrhenius plots. This observation defies the established view that the fast ≈10³ m·s⁻¹ martensite growth must be an athermal (time-independent) process[4,7]. However this is only apparently so, because the thickness of the martensite relates the discharge of the transformation strains into the surrounding austenite. In the case of intrinsic transformation, that is, in the absence of self-accommodation, most of that should depend on the austenite plasticity. It is claimed that the apparent-activation energies above obtained characterize the thermal process that underlies the austenite plasticity and/or the transfer of dislocations into the martensite[40]. As already mentioned the importance of the austenite plasticity on the size of martensite has been brought up in the first half of the XX century[3,4] and, more recently, extended to isothermal martensite[41].

Finally, it is germane to note that the analysis of the intrinsic dimensions of martensite based on the JMAK equations yielded results compatible with previous investigations of the martensite substructure and growth in similar alloys above reviewed.
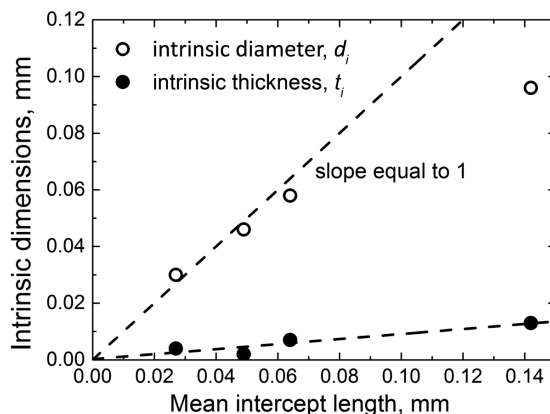

Figure 5. Martensite intrinsic thickness and diameter typical of the initial transformation burst in the Fe-31wt%Ni-0.02wt%C alloy as a function of the austenite grain intercept. The temperatures of the bursts are in the interval 212-222 K. Data from Table 3. The straight lines indicate a linear dependence of both r_i and t_i on d_γ.

6. Summary and Conclusions

In this work the microstructure path method has been, for the first time, applied to the martensite transformation units. New insights on a possible thermal activated step on the martensite transformation could be gained as a result of this novel analysis. The main conclusions are summarized as follows

- The concept of microstructural path has been reviewed and extended to the realm of the martensite transformation.
- The derived microstructural path functions applied to experimental data yielded the intrinsic dimensions of the martensite units formed in Fe-31.1wt%Ni-0.02wt%C and in Fe-1.86wt%C alloys.
- The intrinsic aspect ratio of these martensite products was found to decrease from 0.14 to 0.05 in FeNiC alloy and from 0.04 to 0.02 in FeC alloy.
- The austenite grain size was found to be scale factor for the intrinsic dimensions of martensite units in the Fe-31wt%Ni-0.02wt%C microstructure, coherent with the austenite grain partition trend observed in this alloy.
- The analysis of the intrinsic thickness of martensite units as a function of transformation temperature in Fe-31wt%Ni-0.02wt%C as well as in the Fe-1.86wt%C alloy supports the existence of a thermal activated step. The apparent activation-energies obtained in the Arrhenius plots were in the range of 1.1 10⁻²⁰ - 1.27 10⁻²⁰ J/event, which consistent with dislocation processes.
- We do not attribute this step to a thermal activated *growth* of martensite but to the thermally activated *arrest of the growth* of martensite units owing to the *surrounding austenite plasticity*.

Acknowledgements

References

1. Raghavan V. Formation sequence of plates in isothermal martensite transformation. *Acta Metallurgica*. 1969; 17(10):1299-1303. http://dx.doi.org/10.1016/0001-6160(69)90145-X.

2. Guimarães JRC and Gomes JC. Metallographic study of influence of austenite grain-size on martensite kinetics in Fe-31.9 Ni-0.02C. *Acta Metallurgica*. 1978; 26(10):1591-1596. http://dx.doi.org/10.1016/0001-6160(78)90068-8.

3. Kurdyumov GV. Diffusionless transformation in alloys. *Journal of Technical Physics*. 1948; 18(8):999-1025.

4. Machlin ES and Cohen M. Burst phenomenon in the martensitic transformation. *Transactions AIME*. 1951; 191(9):746-754.

5. Okamoto H, Oka M and Tamura I. Crossings of thin-plate martensites in an Fe-Ni-C alloy. *Acta Metallurgica*. 1979; 27(12):1789-1799. http://dx.doi.org/10.1016/0001-6160(79)90070-1.

6. Bokros JC and Parker ER. Mechanism of martensite burst transformation in Fe-Ni single crystals. *Acta Metallurgica*. 1963; 11(12):1291-1301. http://dx.doi.org/10.1016/0001-6160(63)90024-5.

7. Bunshah RF and Mehl RF. Rate of propagation of martensite. *Transactions AIME*. 1953; 197:1251-1258.

8. Patterson RL and Wayman CM. The crystallography and growth of partially-twinned martensite plates in Fe-Ni alloys. *Acta Metallurgica*. 1966; 14(3):347-369. http://dx.doi.org/10.1016/0001-6160(66)90094-0.

9. Raghavan V and Cohen M. A nucleation model for martensitic transformations in iron-base alloys. *Acta Metallurgica*. 1972; 20(3):779-786. http://dx.doi.org/10.1016/0001-6160(72)90125-3.

10. Christian JW. Thermodynamic and kinetics of martensite. In: Owen WS, editor. *ICOMAT 1979 Proceedings*. Boston: MIT Press; 1979. p. 129-142.

11. Meyers MA. On the growth of lenticular martensite. *Acta Metallurgica*. 1980; 28(6):757-770. http://dx.doi.org/10.1016/0001-6160(80)90153-4.

12. Levitas VI, Idesman AV, Olson GB and Stein E. Numerical modelling of martensitic growth in an elastoplastic material. *Philosophical Magazine A*. 2002; 82(3):429-462. http://dx.doi.org/10.1080/01418610208239609.

13. Olson GB and Cohen M. Principles of martensitic transformation. In: Meyers MA and Inal OT, editors. *Frontiers in materials technologies*. Amsterdam: Elsevier; 1985. p. 43-87.

14. Shibata A, Morito S, Furuhara F and Maki T. Local orientation change inside lenticular martensite plate in Fe–33Ni alloy. *Scripta Materialia*. 2005; 53(5):597-602. http://dx.doi.org/10.1016/j.scriptamat.2005.04.023.

15. Shibata A, Murakami T, Morito S, Furuhara T and Maki T. The origin of midrib in lenticular martensite. *Materials Transactions*. 2008; 49(6):1242-1248. http://dx.doi.org/10.2320/matertrans.MRA2007296.

16. DeHoff RT. Annealing processes: recovery, recrystallization and grain growth. In: Hansen N, Jensen DJ, Leffers T and Ralph B, editors. *Proceedings of the 7th Conference of Risø National Laboratory*; 1986, Roskilde, Denmark. Roskilde: Risø National Laboratory; 1986.

17. Vandermeer RA, Masumura RA and Rath B. Microstructural paths of shape-preserved nucleation and growth transformations. *Acta Metallurgica et Materialia*. 1991; 39(3):383-389. http://dx.doi.org/10.1016/0956-7151(91)90317-T.

18. Rios PR and Guimarães JRC. Microstructural path analysis of athermal martensite. *Scripta Materialia*. 2007; 57(12):1105-1108. http://dx.doi.org/10.1016/j.scriptamat.2007.08.019.

19. Guimarães JRC and Rios PR. Spatial aspects of martensite. *Metallurgical and Materials Transactions. A, Physical Metallurgy and Materials Science*. 2012; 43(7):2218-2224. http://dx.doi.org/10.1007/s11661-012-1102-z.

20. Avrami MJ. Kinetics of phase change I general theory. *The Journal of Chemical Physics*. 1939; 7(12):1103-1112. http://dx.doi.org/10.1063/1.1750380.

21. Johnson WA and Mehl RF. Reaction kinetics in processes of nucleation and growth. *Transactions AIME*. 1939; 135:416-441.

22. Kolmogorov NA. The statistics of crystal growth in metals. *Isvestiia Academii Nauk SSSR - Seriia Matematicheskaia*. 1937; 1:333-359.

23. Rios PR and Villa E. Transformation kinetics for inhomogeneous nucleation. *Acta Materialia*. 2009; 57(4):1199-1208. http://dx.doi.org/10.1016/j.actamat.2008.11.003.

24. Nok Chiu S, Stoyan D, Kendall WS and Mecke J. *Stochastic geometry and its applications*. 3rd ed. UK: John Willey & Sons; 2013.. http://dx.doi.org/10.1002/9781118658222.

25. Cech RE and Turnbull D. Heterogeneous nucleation of the martensite transformation. *Transactions AIME*. 1956; 206(2):124-132.

26. Guimarães JRC and Gomes JC. Microstructural aspects of martensite transformation in coarse-grained Fe-31.1 pct Ni-0.02 pct C. *Metallurgical and Materials Transactions. A, Physical Metallurgy and Materials Science*. 1979; 10(1):109-112. http://dx.doi.org/10.1007/BF02686413.

27. Guimarães JRC and Gomes JC. Martensitic plate dimensions and their relationship to austenitic grain size. In: Owen WS, editor. *ICOMAT-1979 Proceedings*. Boston: MIT Press; 1979. p. 59-64.

28. Guimarães JRC and Brandão LPM. Determination of number and size-distribution of martensitic plates in Fe-31.9%Ni-0.02%C. *Scripta Metallurgica*. 1980; 14(3):305-310. http://dx.doi.org/10.1016/0036-9748(80)90349-X.

29. Menditatta MG and Krauss G. Development of martensitic microstructure and microcracking in an Fe-1.86C alloy. *Metallurgical Transactions*. 1972; 3(7):1755-1760. http://dx.doi.org/10.1007/BF02642557.

30. Samek L, De Moor E, Penning J and De Cooman BC. Strain-induced martensitic nucleation in low-alloy multiphase high-strength steels. *Metallurgical and Materials Transactions. A, Physical Metallurgy and Materials Science*. 2006; 37(1):109-124. http://dx.doi.org/10.1007/s11661-006-0157-0.

31. Fullman RL. Measurement of particle sizes in opaque bodies. *Transactions AIME*. 1953; 197(3):447-452.

32. Datta R and Raghavan V. The semithickness-to-radius ratio of martensitic plates in Fe-Ni alloys. *Materials Science and Engineering A*. 1982; 55(2):239-246. http://dx.doi.org/10.1016/0025-5416(82)90137-9.

33. Visvesvaran P. A study on morphology and plate mean dimensions in Fe-Ni and Fe-Ni-Cr alloys. *Metallurgical and Materials Transactions. A, Physical Metallurgy and Materials Science*. 1996; 27(4):973-980. http://dx.doi.org/10.1007/BF02649765.

34. Stormvinter A, Hedstrom P and Borgenstam A. A transmission electron microscopy study of plate martensite formation in high-carbon low alloy steels. *Journal of Materials Science and Technology*. 2013; 29(4):373-379. http://dx.doi.org/10.1016/j.jmst.2013.01.016.

35. Guimarães JRC and Rios PR. Microstructural analysis of the martensite volume fraction. *Metallurgical and Materials Transactions. A, Physical Metallurgy and Materials Science*. 2013; 44(1):147-151. http://dx.doi.org/10.1007/s11661-012-1506-9.

36. Christian JW and Knowles KW. Interface structures and growth mechanisms. In: Aaronson HI, Laughlin DE, Sekerka RF and Wayman CM, editors. *Proceedings of the international conference on solid-to-solid phase transformations*. Warrendale: TMS-AIME; 1982. p. 1185-1207.

37. Shibata A, Furuhara T and Maki T. Interphase boundary structure and accommodation mechanism of lenticular martensite in Fe–Ni alloys. *Acta Materialia*. 2010; 58(9):3477-3492. http://dx.doi.org/10.1016/j.actamat.2010.02.022.

38. Haezebrouck DM. *Nucleation and growth of a single martensite particle*. [Dissertation]. Cambridge: Massachusetts Institute of Technology; 2005.

39. Raghavan V. The semithickness-to-radius ratio of martensitic plates in iron base alloys. *Scripta Materialia*. 1997; 36(9):995-999. http://dx.doi.org/10.1016/S1359-6462(96)00500-3.

40. Shibata A, Morito S, Furuhara T and Maki T. Substructures of lenticular martensites with different martensite start temperatures in ferrous alloys. *Acta Materialia*. 2009; 57(2):483-492. http://dx.doi.org/10.1016/j.actamat.2008.09.030.

41. Ghosh G and Raghavan V. The dimensions of isothermally formed martensitic plates in an F e-N i-Mn alloy. *Materials Science and Engineering*. 1986; 79(2):223-231. http://dx.doi.org/10.1016/0025-5416(86)90407-6.